Neuron, Vol. 21, 481–493, September, 1998, Copyright ©1998 by Cell Press

A Novel Signaling Pathway from Rod Photoreceptors to Ganglion Cells in Mammalian Retina

Ed Soucy,*§ Yanshu Wang,†§ Sheila Nirenberg,*‖ Jeremy Nathans,†‡ and Markus Meister*#
*Department of Molecular and Cellular Biology
Harvard University
Cambridge, Massachusetts 02138
†Department of Molecular Biology and Genetics
‡Howard Hughes Medical Institute
Johns Hopkins University
School of Medicine
Baltimore, Maryland 21205

Summary

Current understanding suggests that mammalian rod photoreceptors connect only to an ON-type bipolar cell. This rod-specific bipolar cell excites the AII amacrine cell, which makes connections to cone-specific bipolar cells of both ON and OFF type; these, in turn, synapse with ganglion cells. Recent work on rabbit retina has shown that rod signals can also reach ganglion cells without passing through the rod bipolar cell. This route was thought to be provided by electrical gap junctions, through which rods signal directly to cones and thence to cone bipolar cells. Here, we show that the mouse retina also provides a rod pathway bypassing the rod bipolar cell, suggesting that this is a common feature in mammals. However, this alternative pathway does not require cone photoreceptors; it is perfectly intact in a transgenic mouse whose retina lacks cones. Instead, the results can be explained if rods connect directly to OFF bipolar cells.

Introduction

The vertebrate retina senses light with two kinds of photoreceptors (Dowling, 1987; Sterling, 1990). Rods are very sensitive, can reliably transduce the absorption of single photons, and are responsible for vision at low light levels, such as moonlight. Cones are much less sensitive and provide for daytime vision. Both rods and cones hyperpolarize following an increase in light intensity, and thus release less of their transmitter, glutamate. Cones make synapses onto two types of bipolar cells: one type depolarizes following a light increase and is thus called "ON bipolar" or "depolarizing bipolar"; the other type hyperpolarizes in light, the so-called "OFF bipolar" or "hyperpolarizing bipolar." The different responses of ON and OFF bipolar cells are determined by their glutamate receptors: in the OFF bipolar, glutamate causes sodium influx through ionotropic receptors; in the ON bipolar, metabotropic receptors link glutamate to the closure of cation channels (Nawy and Jahr, 1991; Yamashita and Wässle, 1991). This split into two parallel pathways is maintained in subsequent circuitry; ON bipolars excite ON ganglion cells, and OFF bipolars excite OFF ganglion cells. As a result, a transient increase in light intensity is transmitted to the brain by a rapid burst of spikes from ON ganglion cells, whereas a transient decrease in intensity is encoded mostly by a burst of spikes from OFF ganglion cells (Warland et al., 1997).

In the retinae of cold-blooded vertebrates, rod photoreceptors are connected to ON and OFF bipolar cells in much the same fashion as cones. However, in mammals, the circuit for low light vision appears to differ significantly from this plan (Figure 1). It is thought that mammalian rods connect to a single type of bipolar cell (Boycott and Dowling, 1969; Dacheux and Raviola, 1986; Wässle et al., 1991), the rod-depolarizing bipolar (RDB). Following an increase in light intensity, this neuron excites the AII amacrine cell (Kolb and Famiglietti, 1974; Kolb and Nelson, 1983; Chun et al., 1993). The AII cell, in turn, connects to the two classes of cone bipolar cells (Kolb and Famiglietti, 1974; Famiglietti and Kolb, 1975; Pourcho and Goebel, 1985; Müller et al., 1988); it excites cone-depolarizing bipolar (CDB) cells through an electrical junction, and it inhibits cone-hyperpolarizing bipolar (CHB) cells through a glycinergic synapse. Thus, the parallel ON and OFF pathways are established again; both cone bipolar cells respond to rod input and, in turn, convey the signal to the ON and OFF ganglion cells. This circuit diagram for the rod pathway differs in two important respects from the mammalian cone pathway or the rod pathway in cold-blooded vertebrates: there is only one type of rod bipolar cell, and that bipolar cell does not directly contact the retinal ganglion cells.

It has been proposed that rod signals can also travel by another route that circumvents the rod bipolar cell—namely, by passing through gap junctions to cones and from there to the cone ON and OFF bipolar cells. Electrical connections between rod and cone cells have, in fact, been documented both physiologically (Nelson, 1977; Schneeweis and Schnapf, 1995) and anatomically (Smith et al., 1986). Pharmacological experiments also point to a rod pathway bypassing the rod ON bipolar. The glutamate analog L-(+)-2-amino-4-phosphonobutyric acid (APB) acts selectively on metabotropic glutamate receptors, and thus blocks transmission from photoreceptors to ON bipolar cells (Shiells et al., 1981; Slaughter and Miller, 1981; Nawy and Jahr, 1991) but not to OFF bipolar cells (Slaughter and Miller, 1981; Müller et al., 1988). DeVries and Baylor (1995) studied the effects of APB on the rod-driven responses of ganglion cells in the rabbit retina. APB blocked the light response of ON cells, but the function of certain OFF ganglion cells remained intact.

In this paper, we test whether this alternate pathway for rod signals does, in fact, rely on cones. We found that the retina of the mouse provides an APB-resistant pathway for rod signals, as in the rabbit, suggesting that this is a common trait of mammalian retinae. We then removed cones from the mouse retina by molecular genetic methods. Remarkably, the APB-resistant response persisted unaltered in the coneless transgenic retina.

§These authors contributed equally to this work.
‖Present address: Department of Neurobiology, University of California School of Medicine, Los Angeles, California 90095.
#To whom correspondence should be addressed.

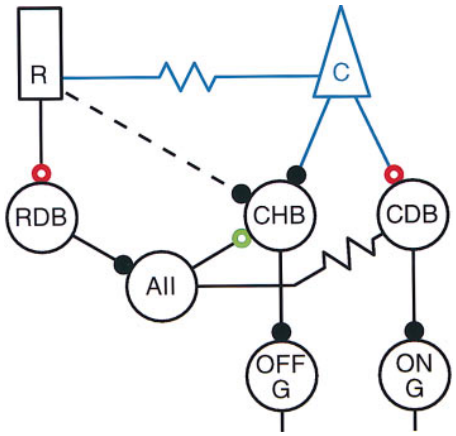

Figure 1. Schematic of the Mammalian Rod and Cone Pathways

The neurons shown are a rod (R), cone (C), rod-depolarizing bipolar (RDB), cone depolarizing bipolar (CDB), cone-hyperpolarizing bipolar (CHB), AII amacrine cell (AII), ON ganglion cell (ON G), and OFF ganglion cell (OFF G). Small filled circles represent sign-preserving synapses, open circles represent sign-inverting synapses, and the "resistor" symbol represents gap junctions. The blue part of the circuit is eliminated in the coneless transgenic mouse, red synapses are blocked by APB, and green synapses are blocked by strychnine. The dashed connection provides a hypothetical rod pathway that is resistant to APB and does not require cones.

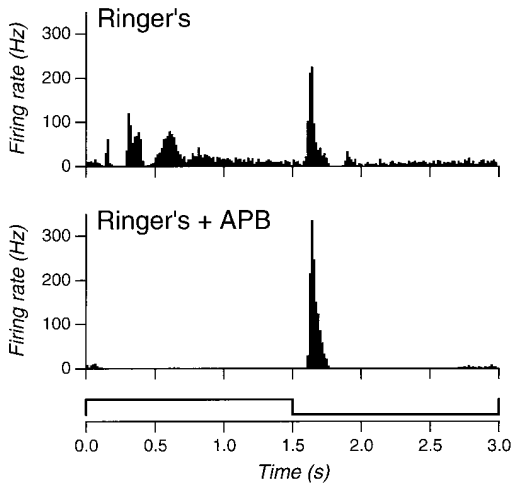

Figure 2. APB Blocks the ON Response but Not the OFF Response of Ganglion Cells

Firing rate of an ON/OFF ganglion cell from the normal mouse retina in response to a spatially uniform square wave flash (bottom stimulus trace) at a mean illumination of 10^2 R*/rod/s and 99% contrast. (Top) In Ringer's solution.
(Bottom) After addition of 100 μM APB.

We conclude that rod–cone coupling is not required and that there is a previously unidentified pathway by which rod signals reach retinal ganglion cells.

Results

The Mouse Retina Has a Pathway for Rod Signals Resistant to APB

The light responses of ganglion cells in the normal mouse retina were tested with a simple stimulus: uniform illumination turned on and off in a square wave fashion (Figure 2). The light intensity was kept in a range that did not activate cones, with the mean intensity producing fewer than 10^2 rhodopsin activations (R*) per rod per second. Many ganglion cells responded with a brief increase in the firing rate at light onset (ON cells), at light offset (OFF cells), or following both transitions (ON/OFF cells; see also Nirenberg and Meister, 1997).

The addition of 100 μM APB eliminated responses to light onset in both ON cells and ON/OFF cells (99 of 99 observed cells), as illustrated in Figure 2. However, OFF responses persisted in both OFF cells and ON/OFF cells (39 of 39 cells), and often their amplitude was enhanced (Figure 2). In darkness or constant dim light (10^2 R*/rod/s), some neurons showed a significant maintained firing rate. APB suppressed this spontaneous activity in ON cells but did not strongly affect it in OFF or ON/OFF cells (data not shown).

To confirm that the APB-resistant responses originate in rod photoreceptors, we measured their spectral sensitivities. For this purpose, recordings were taken from the inferior region of the mouse retina, which contains only short wavelength cones (Szel et al., 1992; Wang et al., 1992) whose absorption spectrum is very different from that of the rods. Reverse correlation to a chromatic random flicker stimulus (see Experimental Procedures and Meister et al., 1994) revealed the relative sensitivities of each ganglion cell to the three guns of the stimulating color monitor (Figure 3A). At low intensities, the green and blue guns were about equally effective in driving these ganglion cells, whereas at high intensities, the blue gun became dominant. The sensitivities to the three guns were interpolated by a standard pigment nomogram (Baylor et al., 1987) to estimate the photoreceptor's peak absorption wavelength (λ_{max}). At intensities below 10^2 R*/rod/s, the λ_{max} clustered tightly around 500 nm (Figure 3B), which is the λ_{max} of the rod photoreceptor, as measured by suction electrode recording (C. Makino, personal communication). When the intensity was increased to 10^6 R*/rod/s, the ganglion cells' spectral sensitivity shifted far toward short wavelengths (Figure 3B). Thus, it appears that low intensities up to 10^2 R*/rod/s stimulate rod photoreceptors exclusively.

Given that the APB-resistant response arises in rods, might it result from an incomplete block of the synapse onto the RDB cell? This is unlikely, because the OFF response persisted at an APB concentration of 600 μM, whereas the ON response was completely eliminated at concentrations of both 100 μM or 600 μM (8 of 8 cells tested). This was observed both at scotopic (10^2 R*/rod/s) and photopic (10^6 R*/rod/s) light intensities.

To further confirm that these OFF responses do not pass through the classical rod pathway, we also tested the effects of strychnine, which interferes with the glycinergic synapse of the AII amacrine cell (Müller et al., 1988) and thus blocks transmission to the cone OFF bipolar cell (Figure 1). However, the APB-resistant response persisted in strychnine (Figure 4; 5 of 5 cells tested). Thus, it appears that rod signals can reach OFF ganglion cells by a route that requires neither the RDB nor the AII amacrine cell.

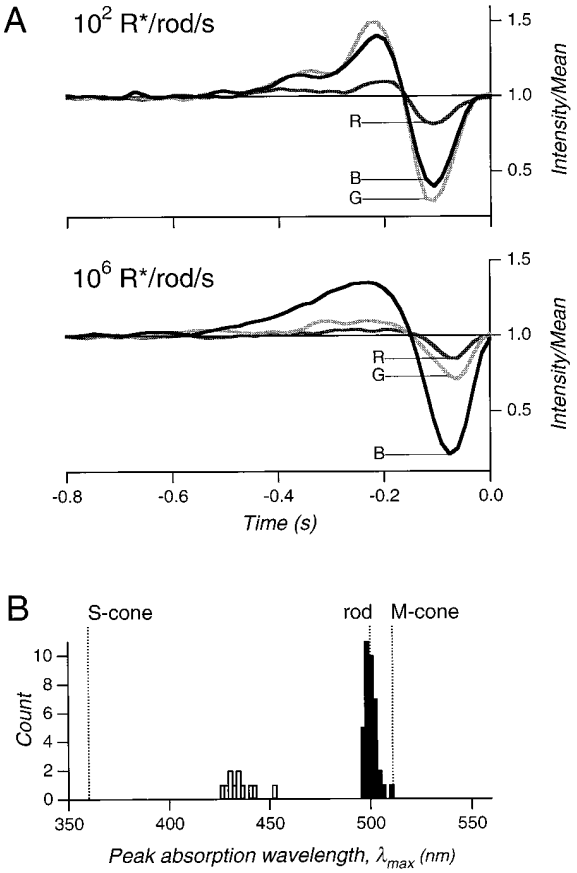

Figure 3. The Spectral Sensitivity of Light Responses in APB

(A) Reverse correlation function of a ganglion cell during two random flicker experiments in 100 μM APB at intensities of 10^2 R*/rod/s (top) and 10^6 R*/rod/s (bottom). In each graph, the three curves represent the spike-triggered average stimulus intensity as a function of time prior to the action potential, plotted separately for the red, green, and blue guns of the color monitor.

(B) From the relative sensitivities to the three guns in (A), the wavelength of peak sensitivity (λ_{max}) of the absorbing photopigment was estimated by using a pigment nomogram (see Experimental Procedures). Solid bars in the histogram show the λ_{max} of 37 ganglion cells at a mean light level of 10^2 R*/rod/s. Open bars show the results obtained at 10^6 R*/rod/s for 11 of these cells. Dashed lines indicate the estimated λ_{max} for the three known photoreceptors: 360 nm (S-cone), 500 nm (rod), and 511 nm (M-cone). All of these recordings were from the inferior region of the mouse retina, which contains S-cones and rods but no M-cones.

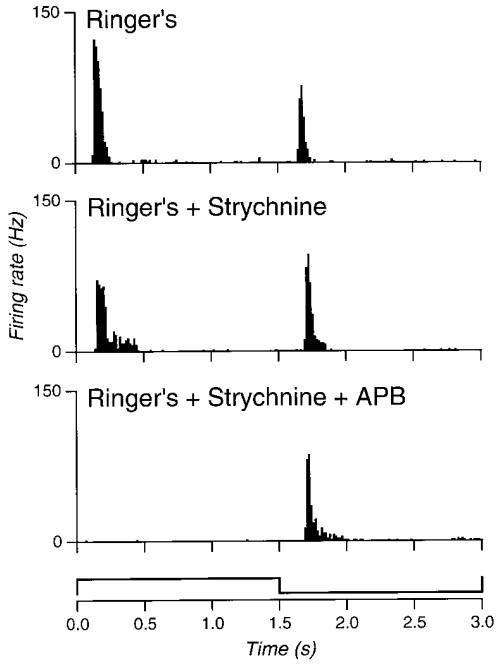

Figure 4. The APB-Resistant Rod Pathway Is Also Resistant to Strychnine

Firing rate of an ON/OFF ganglion cell in response to a square wave flash at intensity 10^2 R*/rod/s and 99% contrast (bottom stimulus trace) measured in Ringer's medium (top), after addition of 13 μM strychnine (middle) and with 13 μM strychnine and 100 μM APB (bottom).

Characteristics of the Two Rod Pathways

We found that individual ganglion cells receive rod signals both through the conventional RDB–AII pathway and through the APB-resistant pathway. However, the relative strength of the two contributions depends strongly on light intensity. At mean intensities below 1 R*/rod/s, APB effectively eliminated all responses of both ON type and OFF type (Figure 5A). This is consistent with responses generated exclusively by the RDB–AII circuit. At intensities greater than 10 R*/rod/s, the APB-resistant OFF response appeared (Figure 5A).

The two OFF response pathways also have differential sensitivity to stimulus contrast. By varying the amplitude of the square wave light stimulus about the mean of 10^2 R*/rod/s, ganglion cell responses could be followed over a wide range of contrasts. For stimuli of 16% contrast or less, the addition of APB greatly attenuated OFF responses. At higher contrasts, APB failed to eliminate OFF responses, and in many instances they were greater than when measured in normal medium (Figure 5B; see also Figure 2).

Thus, the APB-sensitive component of the ganglion cell's OFF response—presumably mediated by the RDB–AII pathway—is dominant at low intensity or low contrast. The APB-resistant OFF pathway requires stimuli of higher mean intensity and contrast, though these still elicit responses exclusively from rods. In this regime, excitation through the alternative pathway may even exceed the contribution from the RDB–AII pathway.

Generation of a Coneless Transgenic Mouse

It has been suggested that the APB-resistant pathway relies on electrical coupling between rods and cones via gap junctions (Smith et al., 1986; DeVries and Baylor, 1995). To test this proposal, we generated a mouse retina in which the cone photoreceptors are selectively missing. This was achieved by expressing the gene for a modified diphtheria toxin under the control of a promoter selective for cones.

Transgenic lines were created that carry a DNA segment encoding the A chain of diphtheria toxin (DT-A) under the control of 6.5 kb of 5′ flanking sequences derived from the human red pigment gene. This region was shown in previous experiments to direct expression

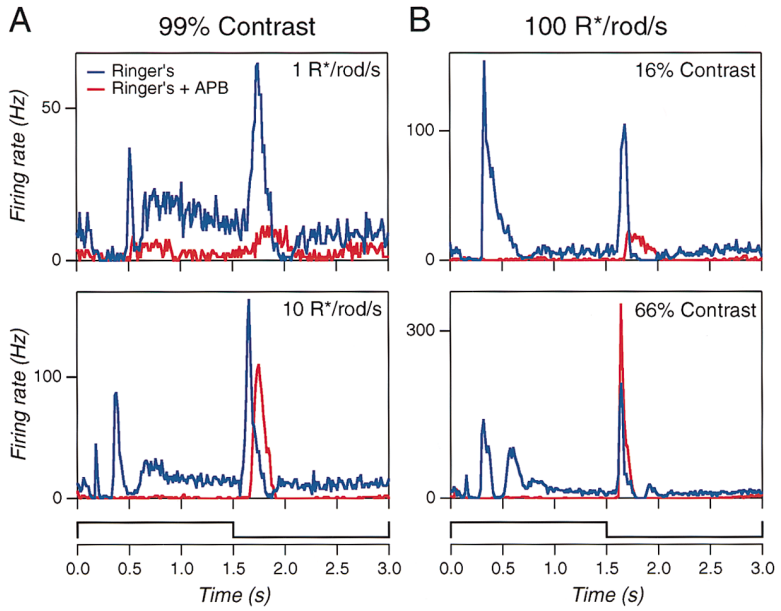

Figure 5. Dependence of the APB-Resistant Rod Response on Intensity and Contrast

Firing rate of an ON/OFF ganglion cell in response to a square wave flash (bottom stimulus trace), in Ringer's medium (blue) and after addition of 100 μM APB (red).

(A) Flashes of 99% contrast, with a mean intensity of 1 R*/rod/s (top) and 10 R*/rod/s (bottom).

(B) Flashes with a mean intensity of 10^2 R*/rod/s, at a contrast of 16% (top) and 66% (bottom).

of a β-galactosidase reporter gene to both long and short wave cones but not to other cell types in the mouse retina (Wang et al., 1992). Our initial attempts to create transgenic lines carrying this construct with a wild-type DT-A coding region resulted in a low yield of transgenic animals. In the three transgenic lines obtained, cone photoreceptor loss was not observed, as determined by crossing the DT-A transgenic mice to mice carrying the same red pigment gene sequences driving expression of a β-galactosidase reporter. Work by others has suggested that leaky expression from DT-A transgenes can result in lethality, thereby enriching within the set of DT-A transgenic lines for those in which the transgene is disrupted or has integrated into a chromosomal region that precludes its expression (Breitman et al., 1990; Lang and Bishop, 1993). To minimize nonspecific cell killing, transgenic animals were generated with a second construct containing the same 6.5 kb red pigment gene segment joined to a DT-A coding segment encoding an attenuated toxin (DT176) (Maxwell et al., 1987; Breitman et al., 1990). With this construct, referred to hereafter as "h.red DT-A," five transgenic lines were obtained, and of these, three showed a nearly complete loss of cone photoreceptors, as determined by crosses with mice carrying the red pigment gene β-galactosidase reporter (Figure 6). H.red DT-A mice show no physical, behavioral, reproductive, or growth anomalies, and the histologic appearance of their retinae remains unchanged over at least 8 months.

Histology of the Coneless Retina

In the normal mouse retina, cones account for fewer than 5% of the photoreceptors and are dispersed among the more numerous rods. As in other rodents, long wave cones are located in the superior retina and short wave cones in the inferior retina (Szel et al., 1992; Wang et al., 1992). Except for differences in chromatin clumping, mouse cones are not morphologically distinctive at the resolution of the light microscope (Carter and LaVail, 1979). H.red DT-A and normal retinae were compared by light and electron microscopy and by a variety of immunochemical probes. Plastic sections (1 μm) (Figures 7M and 7N) show that normal and h.red DT-A retinae were indistinguishable in thickness and in the appearance and arrangement of cellular elements in each of the three retinal layers. Cone photoreceptors were identified by staining with antibodies specific to either long or short wave cone pigments (Wang et al., 1992) and by staining with peanut agglutinin (PNA), a lectin that selectively binds to the extracellular matrix immediately surrounding the cone photoreceptors (Blanks and Johnson, 1983). In keeping with the assessment of cone number determined using a cone-specific β-galactosidase reporter (Figure 6), these experiments revealed a nearly complete absence of long wave cones and a loss of >95% of short wave cones (Figures 7A, 7B, 7E, 7F, 7I, and 7J). The presence of occasional short wave cones in the inferior half of the retina presumably reflects variegated expression of the h.red DT-A transgene in this cell population. This selective variegation may be related to the severalfold lower level of activity of the human red pigment promoter region in short wave cones relative to long wave cones, as judged by the intensity of X-gal staining seen in retinae from the human red promoter–β-galactosidase transgenic mice. Rod density and morphology appeared normal by both light and electron microscopy and by immunostaining with anti-rhodopsin antibodies (data not shown).

The structure of selected cell types in the inner retina was assessed by immunostaining. Antibodies to recoverin label a subset of cone bipolar cells (Milam et al., 1993; Euler and Wässle, 1995), antibodies to protein kinase C (PKC) label rod bipolar cells (Greferath et al., 1990) as well as cone photoreceptors, and antibodies to Thy-1 label ganglion cells (Barnstable and Dräger, 1984). When each of these antibodies was used for immunostaining, the pattern of labeling in the inner retina of normal and h.red DT-A mice appeared indistinguishable

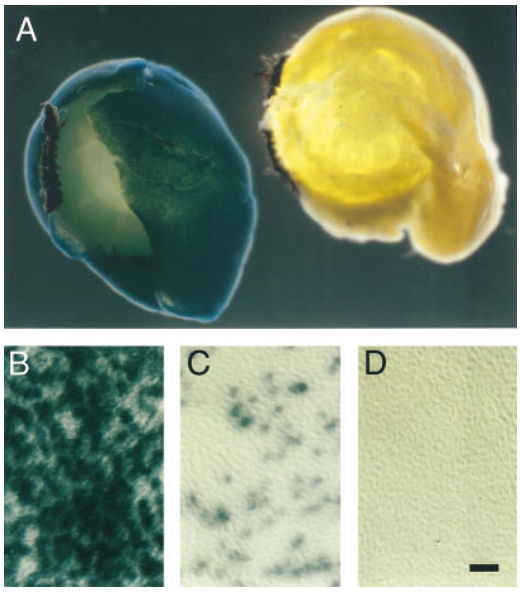

Figure 6. A Transgenic Mouse Retina Almost Entirely Devoid of Cones

Ablation of cone photoreceptors, as assessed using a cone-specific β-galactosidase reporter. Transgenic mice carrying only a human red pigment gene–β-galactosidase reporter ([A], left, and [B]) or double transgenic mice carrying both a human red pigment gene–β-galactosidase reporter and an h.red DT-A transgene ([A], right, [C], and [D]) were examined by whole mount staining with the chromogenic substrate X-gal. Occasional β-galactosidase–expressing cells are seen in the inferior retina of the double transgenic mouse (facing up in [A], right) reaching a density up to 10% of that of the normal retina at the extreme inferior margin (C). In the superior retina of the double transgenic mouse, β-galactosidase–expressing cells are completely absent (D). Scale bar for (B), (C), and (D), 50 μm.

(Figures 7C, 7D, 7G, 7H, 7K, and 7L). In addition, antibodies to calbindin were found to label horizontal cells and their processes, subsets of amacrines, dendrites in three distinct strata of the inner plexiform layer, and neurons in the ganglion cell layer (Schreiner et al., 1985; Hamano et al., 1990). Again, the staining patterns in the normal and coneless retina were indistinguishable (data not shown). Retinae from normal and h.red DT-A mice were also examined by transmission electron microscopy (Figure 8). The qualitative appearances of normal and h.red DT-A retinae are remarkably similar. The only region where any difference could be discerned between the two is in the outer plexiform layer, where occasional large presynaptic swellings with multiple ribbon synapses are found in the normal but not in the h.red DT-A retina. These structures are presumed to be cone pedicles, although this has not been proven by serial reconstruction. The h.red DT-A retina displays the full range of cell types in the inner nuclear and ganglion cell layers, as determined by the morphology and electron density of the cytosol and the pattern of chromatin clumping (Strettoi and Masland, 1995). We conclude that, except for the loss of all long wave cones and nearly all short wave cones, the overall structure of the h.red DT-A retina is remarkably similar to that of the normal mouse. Thus, we will refer to this transgenic retina as a "coneless retina."

The Coneless Retina Is Physiologically Normal at Scotopic Intensities

At scotopic light levels (10^2 R*/rod/s), the light response of the coneless retina was indistinguishable from that of the normal retina. Two types of visual stimuli were used to perform this comparison: spatially uniform square wave flashes and a chromatic randomly flickering checkerboard.

In response to a square wave flash, most ganglion cells of the coneless retina fire brief bursts of spikes at light onset or offset or both, as in the normal retina (Figure 9A). One can distinguish different response types by the timing of these bursts relative to the stimulus period. All of the response types observed in the normal retina also occur in the coneless retina: cells with a short latency single ON response, multiple ON responses, delayed ON responses, and short latency OFF responses (Figure 9A). In fact, the distribution of response types matches quantitatively. For each cell, we measured the peak times for the various elevations in the firing rate throughout the square wave stimulus period. Figure 9B compiles a histogram of these peak times from all of the observed cells. This distribution is very similar in the normal and the coneless retina. This suggests that the coneless retina contains all of the circuitry necessary to generate the scotopic responses of the normal retina.

Ganglion cells of the coneless retina were also characterized by calculating their reverse correlation to a chromatic random flicker stimulus (see Experimental Procedures and Meister et al., 1994). This analysis yields a measure of the ganglion cell's temporal, spatial, and spectral response properties. From the spectral sensitivity, we estimated the λ_{max} of the underlying photoreceptor pigment as $\lambda_{max} = 498 \pm 2$ nm (mean ± SD, 14 cells), which again matches the $\lambda_{max} = 500$ nm of the mouse rod photoreceptor, just as in the normal retina (Figure 3B). Several ganglion cell types could be distinguished by the time course of their reverse correlation (Figure 9C). Most cells showed a biphasic waveform; they varied in the sign of this waveform (ON or OFF type), the particular shape of each lobe, and the occasional occurrence of a third lobe. Examination of 35 cells showed the same qualitative shapes in both the normal and the coneless retina, with no significant difference in their frequency of occurrence. Finally, we measured the size of each ganglion cell's receptive field center by fitting a Gaussian bell shape to the spatial profile of the reverse correlation function (Meister et al., 1995; DeVries and Baylor, 1997). The center diameter (twice the SD of the best fit Gaussian) was 196 ± 58 μm (mean ± SD, 51 cells) in the normal retina and 215 ± 33 μm (14 cells) in the coneless retina, again revealing no significant difference between the two retinae. A diameter of 200 μm corresponds to 8° of visual angle, in good agreement with a typical receptive field size of 10°, measured by others (Stone and Pinto, 1993).

In order to observe any functional difference between the coneless and the normal retina, it was necessary to increase the mean intensity of the stimulus (Figure 10). At an intensity of 10^4 R*/rod/s, the response of the coneless retina was greatly attenuated, and by 10^5 R*/rod/s, there was no detectable response to a square wave stimulus. This occurred in both the inferior and the superior half of

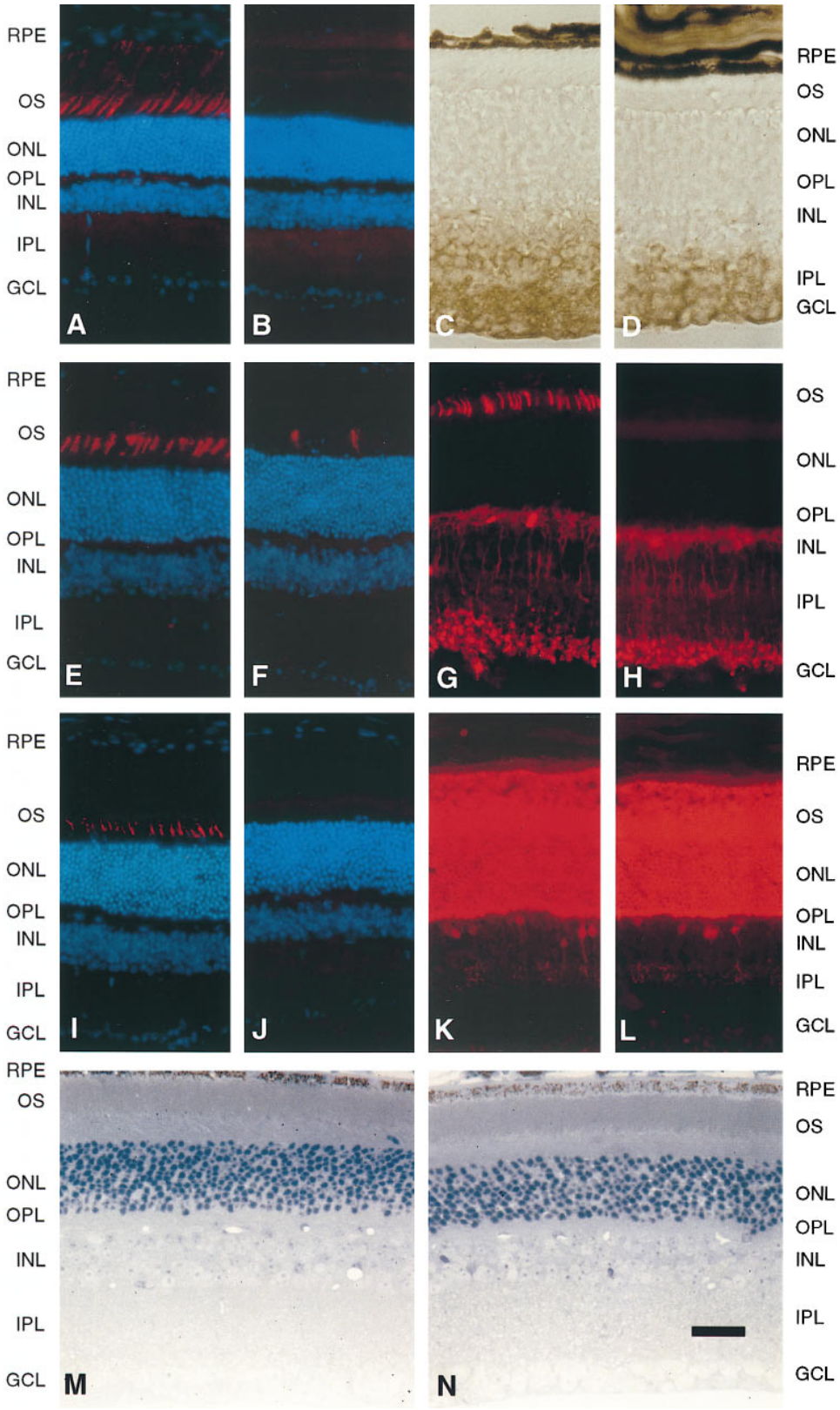

Figure 7. Histology of the Coneless Retina

Light microscopic comparison of h.red DT-A and normal retinae. For each pair of panels, the normal retina is on the left and the h.red DT-A retina is on the right.

(A and B) Double labeling with PNA (red) and DAPI (blue). Cone outer segments and cone-associated extracellular matrix sheaths are presentin the normal retina and absent from the h.red DT-A retina.

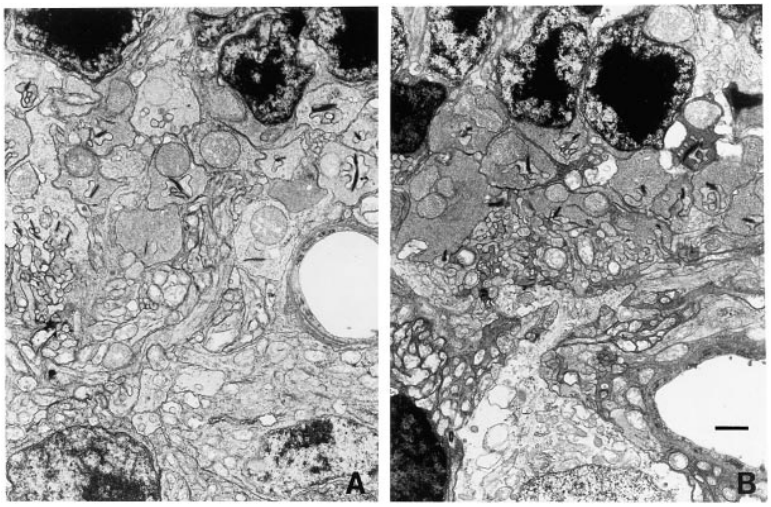

Figure 8. Ultrastructure of the Coneless Retina

Transmission electron microscopy of the outer plexiform layers of normal and h.red DT-A retinae. Photoreceptor nuclei are at the top and nuclei of inner nuclear layer cells are at the bottom. A retinal capillary is on the right side of each micrograph. Both normal (A) and h.red DT-A transgenic (B) retinae show numerous rod spherules with ribbon synapses and invaginating bipolar and horizontal cell processes. The normal sections appear to have a greater number of large presynaptic processes with multiple invaginating synaptic elements, one of which is seen on the left side of (A); these are presumed to be cone pedicles. Scale bar, 1 μm.

the retina. In contrast, the normal retina showed robust responses up to intensities of 10^6 R*/rod/s, the highest value we explored. The failure of the coneless retina at these high intensities is likely the result of saturation of the rod photoreceptors (Nakatani et al., 1991) and serves as a physiological confirmation of the lack of cones.

The Coneless Retina Exhibits an APB-Resistant Response

Having established that the coneless retina functions like the normal retina under scotopic conditions, we tested specifically whether it still has an APB-resistant pathway for rod signals. As in the normal retina (Figures 2 and 5), the addition of 100 μM APB invariably eliminated all ON responses from ganglion cells of the coneless retina (50 of 50 cells tested). However, all cells that showed OFF responses in Ringer's medium continued to respond to light offset in medium containing APB (Figure 11, bottom). Often, the firing transient following light offset was even enhanced over that in Ringer's. This APB-resistant OFF response was observed both in superior retina (7 of 7 cells), which is entirely devoid of cones, and inferior retina (18 of 18 cells), where a small number of cones remains (Figure 6).

To further verify that this response was generated by the same means as in the normal retina, we again tested the effect of APB at various intensities and contrasts. As in the normal retina (Figure 5), APB eliminated both ON and OFF responses at intensities of 1 R*/rod/s or less. However, at intensities >10 R*/rod/s, the APB-resistant response appeared and was often larger than in Ringer's (Figure 11A). The contrast dependence of the APB effect also mirrored that seen in the normal retina; APB attenuated responses to low contrast (16%) flashes, but it failed to suppress responses at higher contrasts (66%) and often enhanced them (Figure 11B).

By all of these measures, it appears that the APB-resistant pathway for rod signals behaves identically in the normal and the coneless retina. Therefore, this pathway clearly does not rely on electrical junctions between rods and cones.

Discussion

Several Pathways for Rod Signals to Ganglion Cells

The current circuit diagram of the mammalian retina (Figure 1) holds that rods synapse onto rod ON bipolar cells, which excite AII amacrine cells, which in turn transmit their signals to both the ON and OFF bipolar cells of the cone circuit. In addition, rod signals may enter cones directly through electrical junctions between the photoreceptors (Sterling, 1990). Here, we have shown that the mouse retina provides yet another pathway from rods to ganglion cells. This pathway bypasses the metabotropic glutamate receptors of ON bipolar cells and

(C and D) Anti-Thy-1 immunostaining visualized with horseradish peroxidase. Ganglion cells and their processes are labeled equivalently in normal and h.red DT-A transgenic retinae.

(E and F) Double labeling of the inferior retina with anti–short wave visual pigment antibodies (red) and DAPI (blue). Occasional short wave cones are seen in the h.red DT-A retina.

(G and H) Anti-PKC immunoreactivity. Rod bipolar cells are stained in both the normal and h.red DT-A transgenic retina; cone outer segments are seen only in the normal retina.

(I and J) Double-labeling of the superior retina with anti–long wave visual pigment antibodies (red) and DAPI (blue). The h.red DT-A transgenic retina shows fewer than 1% of the number of long wave cones seen in the normal retina (none are seen in the h.red DT-A retina section shown here).

(K and L) Anti-recoverin immunoreactivity. Rod photoreceptor cell bodies and outer segments and a subset of cone bipolar cells are immunostained in both normal and h.red DT-A transgenic retinae.

(M and N) Epon-embedded sections (1 μm) stained with methylene blue. Normal and h.red DT-A transgenic retinae are indistinguishable at this resolution. Abbreviations: RPE, retinal pigment epithelium; OS, outer segments; IS, inner segments; ONL, outer nuclear layer; OPL, outer plexiform layer; INL, inner nuclear layer; IPL, inner plexiform layer; GCL, ganglion cell layer. Scale bar, 50 μm.

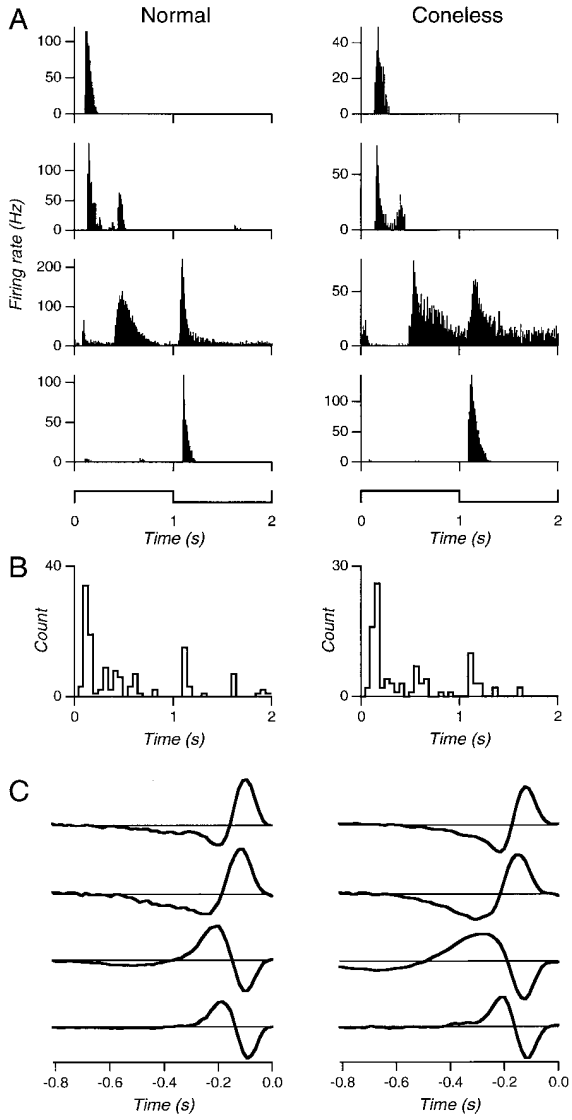

Figure 9. Comparison of Flash Responses in Normal and Coneless Retina

(A) Firing rate as a function of time under periodic square wave flashes at intensity 10^2 R*/rod/s and 99% contrast (bottom stimulus trace) for representative ganglion cells in the normal (left) and coneless (right) retina.

(B) To assess the time course of light responses quantitatively, the times at which the firing rate peaked were noted for every cell (see curves in [A]). These peak times are histogrammed for 68 cells from the normal retina (left) and 61 cells from the coneless retina (right). Cells whose light response showed several peaks (e.g., line 2 in [A]) contributed multiple peak times.

(C) The reverse correlation function to a random checkerboard stimulus for representative cells from the normal (left) and coneless (right) retina. These plots show the spike-triggered average stimulus intensity as a function of time prior to the action potential, obtained as a weighted average of the curves for the red, green, and blue guns (see Figure 3A). All plots are scaled to the same range.

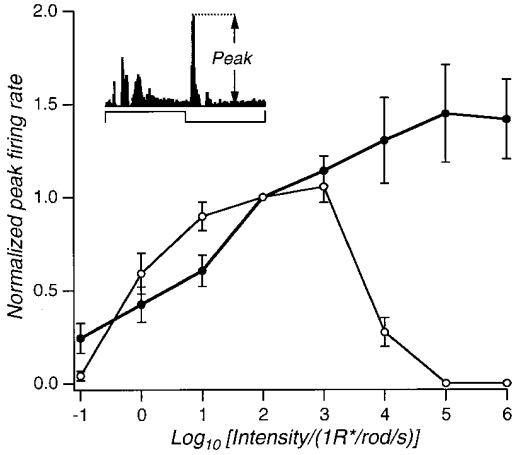

Figure 10. The Coneless Retina Fails at High Light Intensities

The peak firing rate of retinal ganglion cells in response to a square wave stimulus of 99% contrast (see inset) is plotted as a function of the mean intensity over seven orders of magnitude. For each ganglion cell, the peak firing rate was normalized to the value measured at intensity 10^2 R*/rod/s. These normalized values were averaged over 12–18 cells in the normal retina (closed symbols) and 18–27 cells of the coneless retina, including both inferior and superior regions (open symbols). Error bars denote standard error of the mean.

also the glycinergic synapses of AII amacrine cells (Figures 2–4). It is inactive for the weakest light stimuli near the threshold of vision but makes a large contribution to the light response at somewhat higher intensities and contrasts (Figure 5). The pathway does not rely on cones, since it remains intact in a coneless transgenic retina (Figure 11), whose anatomy—with the exception of the loss of cones (Figures 6–8)—and function (Figures 9 and 10) are indistinguishable from the normal retina.

There are several routes by which rod signals could bypass both ON bipolar cells and cones, but most of these can be eliminated based on our observations. For example, horizontal cells may receive inputs from rods and convey the signal laterally to OFF cone bipolars (Linberg and Fisher, 1988; Owen and Hare, 1989; Yang and Wu, 1991). However, horizontal cells are thought to signal by GABAergic transmission, producing a postsynaptic response of the opposite sign (Sarthy and Fu, 1989; Vardi et al., 1994). Thus, OFF ganglion cells should produce ON responses in the presence of APB. Contrary to this expectation, no ON responses were ever observed in APB. Another consideration is that the rod ON bipolar cells express both metabotropic and ionotropic glutamate receptors (Euler et al., 1996; Hughes, 1997). Under normal conditions, metabotropic transduction is dominant, but in the presence of APB, the ionotropic channels could still transmit the rod signal. This would produce an inversion of the postsynaptic response properties, such that in APB, the rod ON bipolar cell turns into an OFF bipolar cell. Thus, ON and OFF ganglion cells should also invert the sign of their response, which was never observed.

A more viable proposal is that the rods directly excite OFF bipolar cells through an ionotropic glutamate receptor. These hypothetical OFF bipolars would excite OFF ganglion cells, whose response would thus be resistant to APB. Under normal conditions, this circuit presumably functions in parallel with the classical rod ON bipolar–AII amacrine circuit. At very low light intensity or low contrast, one expects the RDB–AII circuit

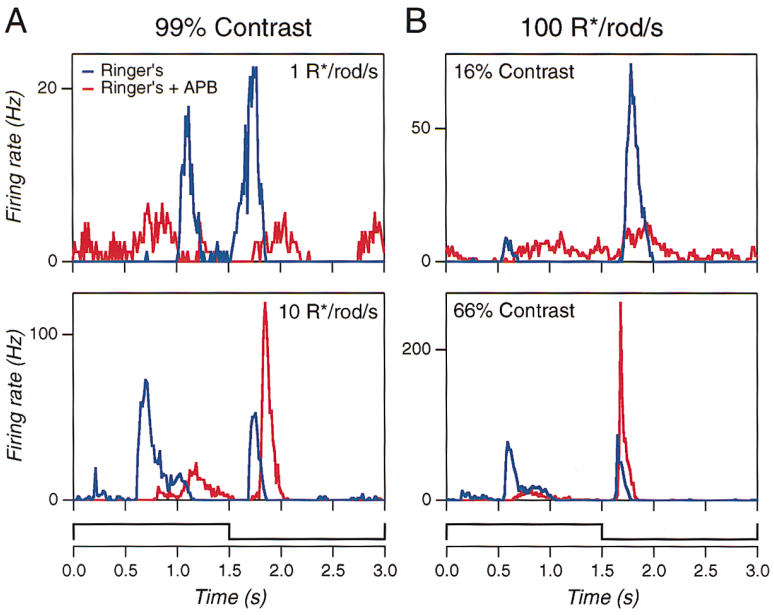

Figure 11. Ganglion Cells of the Coneless Retina Have OFF Responses Resistant to APB

Firing rate of an ON/OFF ganglion cell from the inferior half of a coneless retina in response to a square wave flash (bottom stimulus trace), in Ringer's medium (shaded) and after addition of 100 μM APB (solid line).

(A) Flashes of 99% contrast, with a mean intensity of 1 R*/rod/s (top) and 10 R*/rod/s (bottom).

(B) Flashes with a mean intensity of 10^2 R*/rod/s, at a contrast of 16% (top) and 66% (bottom).

to dominate, owing to the high synaptic gain of the metabotropic glutamate receptor and its signal transduction cascade. Correspondingly, APB eliminated all light responses in this regime (Figure 5A). The same effect was observed previously in the dark-adapted cat retina (Müller et al., 1988). At high intensity and high contrast, one expects that the ionotropic receptor of OFF bipolar cells contributes significantly to transmission. In this regime, APB actually enhanced the response of many OFF ganglion cells (Figure 5B). This can be understood, because APB hyperpolarizes the rod ON bipolar (Yamashita and Wässle, 1991), and thus leads to a reduced glycine release from the AII amacrine cells onto the cone OFF bipolar cell. If this same bipolar cell also receives the excitatory input from rods, transmission of that signal would be facilitated by the reduction of inhibitory input from the AII cell.

Can the Rod Drive an OFF Bipolar Cell?

In this picture, rods and cones connect to the same OFF bipolar cell, as is common in the retinae of cold-blooded vertebrates. Possibly, the RDB–AII circuit is a more recent evolutionary development for the purpose of feeding the sensitive response of the ON bipolar into both ON and OFF ganglion cells (Schiller, 1992). Is it possible that mammals have not altogether discarded the other rod connections?

In cats and primates, it is held that rods connect to only one morphological type of bipolar cell, the "rod bipolar" (Wässle et al., 1991). The primary evidence derives from light microscopy of Golgi-stained retina (Cajal, 1893); in the central area of the retina, the rod spherules are located in a layer clearly distal to the layer of cone pedicles. The only bipolar cells whose dendrites can be seen to reach close to the rod spherules all have a common recognizable morphology (Boycott and Dowling, 1969), and this defines the rod bipolar type. For unknown reasons, cells with this morphology can be labeled selectively with an antibody to PKC (Greferath et al., 1990). This allowed their identification in dissociated cultures, where electrical recording showed them to hyperpolarize in response to glutamate (Yamashita and Wässle, 1991). By combining Golgi or anti-PKC staining with electron microscopy, it was further determined that the rod bipolar dendrites form the central elements in the invaginating synapse of rod spherules (Kolb, 1970; Grünert and Martin, 1991). Thus, it appears well established that cells of the rod bipolar morphology are of the ON type and make invaginating contacts at the rod spherule.

However, it remains possible that rods occasionally connect to other types of bipolar cells. In cat retina, the "flat bipolar" cell receives input from cones and produces an OFF response. Some of the dendrites on these cells project processes vertically into the layer of rod spherules, although no synaptic contacts have been reported there (Boycott and Kolb, 1973). Furthermore, outside of the central retina, rod spherules are intermingled with cone pedicles and thus are far more accessible to "cone bipolar" cells (Boycott and Dowling, 1969). The retina of the squirrel contains two morphological types of bipolar cell that make flat contacts onto both rods and cones (West, 1978). In the retinae of rat or mouse, there have been few studies of the synaptic connectivity of photoreceptors; in fact, the identification of rod bipolars and cone bipolars has relied entirely on the shapes of these neurons and their similarity to bipolar cells in cat and monkey (Euler and Wässle, 1995). However, recent ultrastructural studies of the mouse retina have identified bipolar cell dendrites that form flat contacts with both cone and rod terminals (Y. Tsukamoto, personal communication; see also Muller et al., 1993). These bipolar cells may well mediate the APB-resistant rod pathway described here.

Comparing Coneless and Normal Retina

Both the normal and the coneless retina contain an APB-resistant pathway for transmission of rod signals, but

are they the same pathway? For instance, one might imagine that in the coneless retina, rods connect directly to the (formerly) cone OFF bipolar cells, whereas in the normal retina, rods have electrical junctions with cones, which then connect to cone OFF bipolars. These two pathways to the ganglion cell would be substantially different, in that the latter contains an extra neuron, the cone. In amphibian retina, synaptic transmission is about 10-fold faster at the cone synapse than at the rod synapse (Schnapf and Copenhagen, 1982). While similar measurements are lacking in mammals, one might expect substantially different light responses from the aforementioned two pathways. In contrast, we could not detect any differences in the scotopic light response of the normal and the coneless retina, despite extended efforts to do so (Figures 5, 9, 10, and 11). All of the functional types of ganglion cells are present in both normal and coneless retina, and in the same proportions. Furthermore, by immunostaining and electron microscopy, we found no indication that the structure of the coneless retina was significantly perturbed (Figures 7 and 8).

Nevertheless, we cannot entirely rule out that some rearrangement of rod circuits occurred subsequent to cone ablation and happens to perfectly emulate the function of a different rod pathway in normal retina. Clearly, it would be valuable to confirm the proposed synapse between rods and OFF bipolars, for example, by serial reconstruction of the outer retina. Given the general lack of information about the rodent's photoreceptor connections (Euler and Wässle, 1995) and the growing attraction of molecular genetics in the mouse, such an ultrastructure effort would offer high rewards.

Function of the Rod and Cone Systems

The coneless retina provides a unique opportunity to observe the rod system at high light intensities, where cone signals would normally begin to dominate. Figure 10 shows that the rod system operates over about four orders of magnitude of light intensity. From 10^1–10^3 R*/rod/s, the response of ganglion cells to these square wave flashes was remarkably constant. In these experiments, the mean light intensity increases in proportion with the flash intensity. Thus, a constant light response implies that the flash sensitivity varies in inverse proportion to the mean intensity, a relationship known as Weber-law adaptation (Shapley and Enroth-Cugell, 1984). Recordings of the photocurrent of mammalian rods have documented such Weber-law adaptation in the gain of the flash response over about two orders of magnitude (Yau, 1994). At higher intensities, the phototransduction cascade can no longer adjust, the membrane conductance shuts off, and the rod response disappears. In rat rods, this saturation occurs at $\sim 4 \times 10^3$ R*/rod/s (Nakatani et al., 1991), precisely where the ganglion cell response disappears in the coneless mouse retina (Figure 10). Thus, the upper intensity range of the rod system is likely controlled by gain changes in the photoreceptors rather than "network adaptation" in subsequent circuits (Shapley and Enroth-Cugell, 1984).

At intensities above 10^5 R*/rod/s, the ganglion cell response is due entirely to cone signals (Figure 10). In this regime, ganglion cells of the superior retina were most sensitive in the green ($\lambda_{max} \approx 510$ nm) and those of the inferior retina in the blue ($\lambda_{max} \approx 430$ nm) region of the spectrum (Figure 3B). This is consistent with the well-documented segregation of middle and short wave pigments into superior and inferior retina, respectively (Szel et al., 1992; Wang et al., 1992; Chiu and Nathans, 1994). However, the spectral sensitivity we measured in inferior retina conflicts with the current estimate of the short wave pigment absorption spectrum, which places the absorption maximum in the ultraviolet ($\lambda_{max} \approx 360$ nm). This was derived from measurements of the electroretinogram under full field flicker (Jacobs et al., 1991). Subsequent experiments using focal illumination suggested that the inferior retina was most sensitive in the blue, not the ultraviolet (Calderone and Jacobs, 1995); the discrepancy was blamed on technical problems with light scattering into the superior retina. Here, we show instead that individual ganglion cells in an isolated piece of inferior retina have a spectral sensitivity in the blue rather than the ultraviolet region. Either the proposed short wave cone absorption spectrum is in error, or the inferior retina contains in addition a longer wavelength pigment that is not recognized by the antibodies currently in use. The issue could be resolved by direct recording from cone photoreceptors.

Development of the Coneless Retina

It is thought that the developmental fate of retinal neurons is determined primarily by cell–cell interactions rather than by their lineage (Holt et al., 1988; Adler and Hatlee, 1989; Turner et al., 1990; Watanabe and Raff, 1990). Those cells that exit the mitotic cycle at earlier times are presumed to play an instructive role in determining the fates of cells that are born later (Cepko et al., 1996). Although cones are among the earliest postmitotic cells in the mouse retina (Young, 1985), the experiments reported here suggest that cones may not play a significant role in determining or maintaining the developmental fates of other retinal cell types. This inference should be made with some caution, because the developmental time course of cone cell death in the h.red DT-A transgenic retina has not yet been determined. Even if cone cell death were found to occur at postnatal days 0–3 (P0–P3), when cone pigment expression is first detectable (Wang et al., 1992; Chiu and Nathans, 1994), the nearly normal appearance and function of the h.red DT-A retina could result from an early and transient interaction between cones and developing inner retinal cells. Still, the cones do not appear to be essential for maintaining the neurons that were destined to become cone bipolar cells. In the rat retina, $\sim$50% of bipolar cells are estimated to be cone bipolars, based on their morphology (Euler and Wässle, 1995). If this fraction is similar in the mouse retina, then most of these neurons still exist in the h.red DT-A transgenic mouse, since the inner nuclear layers of normal and h.red DT-A transgenic retinae are indistinguishable in thickness, overall appearance, number of cells, and number of cells staining with anti-recoverin, which labels a subset of cone bipolars. Our recordings in very dim light suggest further that these "coneless" cone-bipolar cells are still

connected to AII amacrines, just as in the normal retina. Presumably, these inputs, along with the direct rod input postulated above, are sufficient to stabilize these bipolar cells.

Additional evidence that the rod pathways remain intact even in the absence of cones comes from human patients suffering from cone degeneration. These patients can have normal rod vision—assessed by psychophysical detection thresholds, the scotopic electroretinogram, and the time course of dark adaptation—without any detectable cone function (Berson et al., 1968). In at least one such case, histology of the autopsy eyes confirmed extensive degeneration of cones in most of the retina (To et al., 1998). Thus, maintenance of the circuitry for rod signals does not require cone function or even the presence of cone inner segments. If rod signals are indeed carried to ganglion cells by bipolar cells with a dominant cone input, then these bipolar cells clearly do not degenerate once the cones are removed.

Conclusion

The present work addresses a common problem in systems neuroscience, namely to explain the function of a large neuronal circuit in terms of its component neurons and their interconnections. In this effort, it is often helpful to perturb the circuit in specific ways while monitoring the effect on overall function. The experimental approach reported here—multineuron recordings combined with genetically engineered ablation of specific neuronal types—should be broadly applicable to the study of signal processing within the central nervous system.

Experimental Procedures

Recording of Ganglion Cell Action Potentials

Spike trains were recorded extracellularly from the ganglion cell layer with a multielectrode array as described previously (Meister et al., 1994; Nirenberg and Meister, 1997). "Normal" mice were females from strain C57Bl/6J, and "coneless" mice are described below. The animals were dark adapted for at least 1 hr prior to enucleation. The retina was isolated into oxygenated Ringer's (110 mM NaCl, 2.5 mM KCl, 1 mM $CaCl_2$, 1.6 mM $MgCl_2$, and 10 mM D-glucose buffered with 22 mM $NaHCO_3$ and 5% CO_2/95% O_2 [pH 7.4]) under infrared illumination. A piece of retina 2–3 mm on a side was cut from the periphery and placed ganglion cell side down on an array of 61 electrodes spaced 70 μm apart. The isolated retina was continuously superfused with oxygenated Ringer's (1 ml/min) and maintained at 35°C. All recordings remained stable for at least 4 hr.

Stimulation

A computer monitor (Apple RGB Display) or the combination of an LCD panel (Sharp QA-1750) and overhead projector (Eiki OHP-4100) were used to deliver visual stimuli that were then imaged onto the photoreceptor surface of the retina. For periodic flash stimuli, the screen was uniformly lit, and the intensity varied in a square wave fashion, with a contrast (on − off)/(on + off) = 0.99, unless noted differently. For random flicker stimuli, the field was divided in a checkerboard of 105 μm square size. In each square, each of the three guns was turned on or off by an independent random choice. These assignments were randomized every 30 ms, yielding a checkerboard flickering rapidly with eight different colors (Meister et al., 1994).

All stimulus intensities are expressed in terms of the time-average rate of photoisomerizations in a rod. To calculate this, the spectral power of visual stimuli was measured with a broad-band photometer (UDT Instruments 350) and a spectrometer (Photo Research PR-650) scanning from 380–780 nm in 4 nm steps. From this emission spectrum and the known spectral sensitivity of the mouse rod (C. Makino, personal communication), we determined the rate of photoisomerizations, assuming in addition that the mouse rod has an optical density at the peak absorption wavelength (λ_{max}) of 0.015 μm^{-1}, a length of 24 μm, a diameter of 1.4 μm, and a quantum efficiency of 0.67 (Carter and LaVail, 1979; Penn and Williams, 1984).

Analysis

In experiments with square wave flashes, we calculated the ganglion cell's average firing rate as a function of time during the stimulus period by histogramming its spike times relative to light onset. In random flicker experiments, we calculated the average visual stimulus as a function of time preceding the cell's action potential: the spike-triggered average intensity of each gun in each pixel at various times preceding the spike (Reid and Shapley, 1992; Meister et al., 1994). This function, also called the "reverse correlation," reveals what features of the visual input are effective in triggering a spike. Its spatial profile shows the cell's receptive field, its time dependence reflects the time course of the cell's neural integration, and the contributions from the three guns of the monitor indicate the cell's relative sensitivity to these three lights.

The relative sensitivity to the three guns of the monitor was used to estimate a ganglion cell's spectral sensitivity. To identify the underlying photoreceptor absorption spectrum, the three measurements were interpolated by a nomogram (Baylor et al., 1987) that fits the shape of pigment spectra in many species. The peak absorption wavelength (λ_{max}) quoted is the λ_{max} of the nomogram providing the best fit.

Pharmacology

All pharmacological agents were dissolved in oxygenated Ringer's solution and were delivered to the retina by continuous superfusion. APB and strychnine were purchased from Sigma.

Transgenic Mice

The DT-A constructs contain 6.5 kb of human red pigment gene 5′ flanking sequence, the 3′ end of which coincides with the initiator methionine codon as described previously (Wang et al., 1992). This segment was fused either to a 0.6 kb wild-type DT-A coding region followed by a 0.5 kb mouse protamine-1 gene intron and polyadenylation site or to a 0.6 kb DT-A 176 (attenuated DT-A) coding region followed by a 0.8 kb fragment containing an SV-40 early region intron and polyadenylation site (Breitman et al., 1990). The inserts were gel purified free of *E. coli* vector sequences and injected into fertilized mouse eggs (DNX). Founders were backcrossed to C57/Bl6 and genotyped by transgene-specific PCR reactions.

Histology and Immunohistochemistry

For light microscopy, enucleated eyes were fixed in 4% paraformaldehyde in phosphate buffered saline (PBS) with 2 mM $MgCl_2$ at 4°C for 30 min. Corneas and lenses were removed and the eyecups further fixed in 4% paraformaldehyde in PBS for 3 hr at 4°C, cryoprotected in 30% sucrose overnight at 4°C, embedded in OCT, and sectioned at 10 μm. Tissue sections were incubated in 5% normal goat serum in PBS with 2 mM $MgCl_2$ and 0.3% Triton X-100 for 1 hr at room temperature followed by incubation at 4°C overnight in primary antibody in the same buffer. The appropriate biotinylated secondary antibody and Texas red–conjugated streptavidin or biotinylated horseradish peroxidase (Vector Laboratories) were used to visualize immunostaining. For PNA staining, tissue sections were incubated with rhodamine-conjugated PNA at room temperature for 1 hr, washed in PBS, mounted in VECTASHIELD mounting solution, and immediately photographed. Reagents were obtained from the following sources: anti-PKC mAb MC5 (Sigma); anti-Thy-1 mAb 1294 (Chemicon); affinity-purified rabbit anti-recoverin polyclonal antibody (Drs. Alexander Dizhoor and James Hurley); rabbit anti–short wave and rabbit anti–long wave cone pigment antibodies (Wang et al., 1992); biotinylated goat anti-rabbit antibody (Vector Laboratories); biotinylated goat anti-mouse antibody (Vector Laboratories); and rhodamine-conjugated PNA (Vector Laboratories).

Plastic Embedding and Electron Microscopy

Semithin and ultrathin sections of retinae were prepared as described in Martinou et al. (1994), with the following modifications. Animals were perfused transcardially with PBS followed by 2% paraformaldehyde and 2% glutaraldehyde in PBS. Tissues were postfixed overnight at 4°C in the same fixative, and following three 10 min rinses in 50 mM sodium cacodylate, they were postfixed at 4°C for 2 hr in 1% osmium tetroxide in 50 mM sodium cacodylate. The fixed tissues were then rinsed in 50 mM sodium cacodylate, dehydrated in graded ethanol solutions, and infiltrated and embedded in epoxy resin. Semithin (1 μm) sections were stained with methylene blue for light microscopy, and ultrathin (0.1 μm) sections were stained with uranyl acetate and lead citrate for electron microscopy.

Acknowledgments

Thanks to Alexander Dizhoor for anti-recoverin antibodies and to Hui Sun, David Caulkins, and Stewart Hendry for helpful advice. This work was supported by a Pew Scholarship and a Presidential Faculty Fellows Award (M. M.), a National Research Service Award (S. N.), and the National Eye Institute (National Institutes of Health) and the Howard Hughes Medical Institute (J. N.).

Received March 20, 1998; revised July 8, 1998.

References

Adler, R., and Hatlee, M. (1989). Plasticity and differentiation of embryonic retinal cells after terminal mitosis. Science *243*, 391–393.

Barnstable, C.J., and Dräger, U.C. (1984). Thy-1 antigen: a ganglion cell specific marker in rodent retina. Neuroscience *11*, 847–855.

Baylor, D.A., Nunn, B.J., and Schnapf, J.L. (1987). Spectral sensitivity of cones of the monkey *Macaca fascicularis*. J. Physiol. (Lond.) *390*, 145–160.

Berson, E.L., Gouras, P., and Gunkel, R.D. (1968). Progressive cone degeneration, dominantly inherited. Arch. Ophthalmol. *80*, 77–83.

Blanks, J.C., and Johnson, L.V. (1983). Selective lectin binding of the developing mouse retina. J. Comp. Neurol. *221*, 31–41.

Boycott, B.B., and Dowling, J.E. (1969). Organization of the primate retina: light microscopy. Philos. Trans. R. Soc. Lond. B Biol. Sci. *255*, 109–184.

Boycott, B.B., and Kolb, H. (1973). The connections between bipolar cells and photoreceptors in the retina of the domestic cat. J. Comp. Neurol. *148*, 91–114.

Breitman, M.L., Rombola, H., Maxwell, I.H., Klintworth, G.K., and Bernstein, A. (1990). Genetic ablation in transgenic mice with an attenuated diphtheria toxin A gene. Mol. Cell. Biol. *10*, 474–479.

Cajal, S.R. (1893). La rétine des vertèbres. La Cellule *9*, 119–255.

Calderone, J.B., and Jacobs, G.H. (1995). Regional variations in the relative sensitivity to UV light in the mouse retina. Visual Neurosci. *12*, 463–468.

Carter, D.L., and LaVail, M.M. (1979). Rods and cones in the mouse retina. I. Structural analysis using light and electron microscopy. J. Comp. Neurol. *188*, 245–262.

Cepko, C.L., Austin, C.P., Yang, X., Alexiades, M., and Ezzeddine, D. (1996). Cell fate determination in the vertebrate retina. Proc. Natl. Acad. Sci. USA *93*, 589–595.

Chiu, M.I., and Nathans, J. (1994). A sequence upstream of the mouse blue visual pigment gene directs blue cone-specific transgene expression in mouse retinas. Vis. Neurosci. *11*, 773–780.

Chun, M.H., Han, S.H., Chung, J.W., and Wässle, H. (1993). Electron microscopic analysis of the rod pathway of the rat retina. J. Comp. Neurol. *332*, 421–432.

Dacheux, R.F., and Raviola, E. (1986). The rod pathway in the rabbit retina: a depolarizing bipolar and amacrine cell. J. Neurosci. *6*, 331–345.

DeVries, S.H., and Baylor, D.A. (1995). An alternative pathway for signal flow from rod photoreceptors to ganglion cells in mammalian retina. Proc. Natl. Acad. Sci. USA *92*, 10658–10662.

DeVries, S.H., and Baylor, D.A. (1997). Mosaic arrangement of ganglion cell receptive fields in rabbit retina. J. Neurophysiol. *78*, 2048–2060.

Dowling, J.E. (1987). The retina: an Approachable Part of the Brain (Cambridge, MA: Harvard University Press).

Euler, T., and Wässle, H. (1995). Immunocytochemical identification of cone bipolar cells in the rat retina. J. Comp. Neurol. *361*, 461–478.

Euler, T., Schneider, H., and Wässle, H. (1996). Glutamate responses of bipolar cells in a slice preparation of the rat retina. J. Neurosci. *16*, 2934–2944.

Famiglietti, E.J., and Kolb, H. (1975). A bistratified amacrine cell and synaptic circuitry in the inner plexiform layer of the retina. Brain Res. *84*, 293–300.

Greferath, U., Grünert, U., and Wässle, H. (1990). Rod bipolar cells in the mammalian retina show protein kinase C–like immunoreactivity. J. Comp. Neurol. *301*, 433–442.

Grünert, U., and Martin, P.R. (1991). Rod bipolar cells in the macaque monkey retina: immunoreactivity and connectivity. J. Neurosci. *11*, 2742–2758.

Hamano, K., Kiyama, H., Emson, P.C., Manabe, R., Nakauchi, M., and Tohyama, M. (1990). Localization of two calcium binding proteins, calbindin (28 kD) and parvalbumin (12 kD), in the vertebrate retina. J. Comp. Neurol. *302*, 417–424.

Holt, C.E., Bertsch, T.W., Ellis, H.M., and Harris, W.A. (1988). Cellular determination in the Xenopus retina is independent of lineage and birth date. Neuron *1*, 15–26.

Hughes, T.E. (1997). Are there ionotropic glutamate receptors on the rod bipolar cell of the mouse retina? Vis. Neurosci. *14*, 103–109.

Jacobs, G.H., Neitz, J., and Deegan, J.F.I. (1991). Retinal receptors in rodents maximally sensitive to ultraviolet light. Nature *353*, 655–656.

Kolb, H. (1970). Organization of the outer plexiform layer of the primate retina: electron microscopy of Golgi-impregnated cells. Philos. Trans. R. Soc. Lond. B Biol. Sci. *258*, 261–283.

Kolb, H., and Famiglietti, E.V. (1974). Rod and cone pathways in the inner plexiform layer of cat retina. Science *186*, 47–49.

Kolb, H., and Nelson, R. (1983). Rod pathways in the retina of the cat. Vision Res. *23*, 301–312.

Lang, R.A., and Bishop, J.M. (1993). Macrophages are required for cell death and tissue remodeling in the developing mouse eye. Cell *74*, 453–462.

Linberg, K.A., and Fisher, S.K. (1988). Ultrastructural evidence that horizontal cell axon terminals are presynaptic in the human retina. J. Comp. Neurol. *268*, 281–297.

Martinou, J.C., Dubois, D.M., Staple, J.K., Rodriguez, I., Frankowski, H., Missotten, M., Albertini, P., Talabot, D., Catsicas, S., Pietra, C., and Huarte, J. (1994). Overexpression of BCL-2 in transgenic mice protects neurons from naturally occurring cell death and experimental ischemia. Neuron *13*, 1017–1030.

Maxwell, F., Maxwell, I.H., and Glode, L.M. (1987). Cloning, sequence determination, and expression in transfected cells of the coding sequence for the tox 176 attenuated diphtheria toxin A chain. Mol. Cell. Biol. *7*, 1576–1579.

Meister, M., Pine, J., and Baylor, D.A. (1994). Multi-neuronal signals from the retina: acquisition and analysis. J. Neurosci. Methods *51*, 95–106.

Meister, M., Lagnado, L., and Baylor, D.A. (1995). Concerted signaling by retinal ganglion cells. Science *270*, 1207–1210.

Milam, A.H., Dacey, D.M., and Dizhoor, A.M. (1993). Recoverin immunoreactivity in mammalian cone bipolar cells. Vis. Neurosci. *10*, 1–12.

Müller, F., Wässle, H., and Voigt, T. (1988). Pharmacological modulation of the rod pathway in the cat retina. J. Neurophysiol. *59*, 1657–1672.

Muller, J.F., Lukasiewicz, P.D., and Silverman, M.S. (1993). Rod and cone inputs to bipolar cells in the rat retina. Invest. Ophthalmol. Vis. Sci. *34* (suppl.), 984.

Nakatani, K., Tamura, T., and Yau, K.W. (1991). Light adaptation in retinal rods of the rabbit and two other nonprimate mammals. J. Gen. Physiol. *97*, 413–435.

Nawy, S., and Jahr, C.E. (1991). cGMP-gated conductance in retinal

bipolar cells is suppressed by the photoreceptor transmitter. Neuron *7*, 677–683.

Nelson, R. (1977). Cat cones have rod input: a comparison of the response properties of cones and horizontal cell bodies in the retina of the cat. J. Comp. Neurol. *172*, 109–135.

Nirenberg, S.A., and Meister, M. (1997). The light response of retinal ganglion cells is truncated by a displaced amacrine circuit. Neuron *18*, 637–650.

Owen, W.G., and Hare, W.A. (1989). Signal transfer from photoreceptors to bipolar cells in the retina of the tiger salamander. Neurosci. Res. *10* (suppl.), 77–87.

Penn, J.S., and Williams, T.P. (1984). A new microspectrophotometric method for measuring absorbance of rat photoreceptors. Vision Res. *24*, 1673–1676.

Pourcho, R.G., and Goebel, D.J. (1985). A combined Golgi and autoradiographic study of (^{3}H)glycine-accumulating amacrine cells in the cat retina. J. Comp. Neurol. *233*, 473–480.

Reid, R.C., and Shapley, R.M. (1992). Spatial structure of cone inputs to receptive fields in primate lateral geniculate nucleus. Nature *356*, 716–718.

Sarthy, P.V., and Fu, M. (1989). Localization of L-glutamic acid decarboxylase mRNA in cat retinal horizontal cells by in situ hybridization. J. Comp. Neurol. *288*, 593–600.

Schiller, P.H. (1992). The ON and OFF channels of the visual system. Trends Neurosci. *15*, 86–92.

Schnapf, J.L., and Copenhagen, D.R. (1982). Differences in the kinetics of rod and cone synaptic transmission. Nature *296*, 862–864.

Schneeweis, D.M., and Schnapf, J.L. (1995). Photovoltage of rods and cones in the macaque retina. Science *268*, 1053–1056.

Schreiner, D.S., Jande, S.S., and Lawson, D.E. (1985). Target cells of vitamin D in the vertebrate retina. Acta Anat. *121*, 153–162.

Shapley, R., and Enroth-Cugell, C. (1984). Visual adaptation and retinal gain controls. Prog. Retinal Res. *3*, 263–346.

Shiells, R.A., Falk, G., and Naghshineh, S. (1981). Action of glutamate and aspartate analogues on rod horizontal and bipolar cells. Nature *294*, 592–594.

Slaughter, M.M., and Miller, R.F. (1981). 2-amino-4-phosphonobutyric acid: a new pharmacological tool for retina research. Science *211*, 182–185.

Smith, R.G., Freed, M.A., and Sterling, P. (1986). Microcircuitry of the dark-adapted cat retina: functional architecture of the rod–cone network. J. Neurosci. *6*, 3505–3517.

Sterling, P. (1990). Retina. In The Synaptic Organization of the Brain, G.M. Shepherd, ed. (New York: Oxford University Press), pp. 170–213.

Stone, C., and Pinto, L.H. (1993). Response properties of ganglion cells in the isolated mouse retina. Vis. Neurosci. *10*, 31–39.

Strettoi, E., and Masland, R.H. (1995). The organization of the inner nuclear layer of the rabbit retina. J. Neurosci. *15*, 875–888.

Szel, A., Rohlich, P., Caffe, A.R., Juliusson, B., Aguirre, G., and Van, V.T. (1992). Unique topographic separation of two spectral classes of cones in the mouse retina. J. Comp. Neurol. *325*, 327–342.

To, K.W., Adamian, M., Jakobiec, F.A., and Berson, E.L. (1998). Histopathologic and immunohistochemical study of an autopsy eye with X-linked cone degeneration. Arch. Ophthalmol. *116*, 100–103.

Turner, D.L., Snyder, E.Y., and Cepko, C.L. (1990). Lineage-independent determination of cell type in the embryonic mouse retina. Neuron *4*, 833–845.

Vardi, N., Kaufman, D.L., and Sterling, P. (1994). Horizontal cells in cat and monkey retina express different isoforms of glutamic acid decarboxylase. Vis. Neurosci. *11*, 135–142.

Wang, Y., Macke, J.P., Merbs, S.L., Zack, D.J., Klaunberg, B., Bennett, J., Gearhart, J., and Nathans, J. (1992). A locus control region adjacent to the human red and green visual pigment genes. Neuron *9*, 429–440.

Warland, D.K., Reinagel, P., and Meister, M. (1997). Decoding visual information from a population of retinal ganglion cells. J. Neurophysiol. *78*, 2336–2350.

Wässle, H., Yamashita, M., Greferath, U., Grünert, U., and Müller, F. (1991). The rod bipolar cell of the mammalian retina. Vis. Neurosci. *7*, 99–112.

Watanabe, T., and Raff, M.C. (1990). Rod photoreceptor development in vitro: intrinsic properties of proliferating neuroepithelial cells change as development proceeds in the rat retina. Neuron *4*, 461–467.

West, R.W. (1978). Bipolar and horizontal cells of the gray squirrel retina: Golgi morphology and receptor connections. Vision Res. *18*, 129–136.

Yamashita, M., and Wässle, H. (1991). Responses of rod bipolar cells isolated from the rat retina to the glutamate agonist 2-amino-4-phosphonobutyric acid (APB). J. Neurosci. *11*, 2372–2382.

Yang, X.L., and Wu, S.M. (1991). Feedforward lateral inhibition in retinal bipolar cells: input–output relation of the horizontal cell–depolarizing bipolar cell synapse. Proc. Natl. Acad. Sci. USA *88*, 3310–3313.

Yau, K.W. (1994). Phototransduction mechanism in retinal rods and cones. The Friedenwald lecture. Invest. Ophthalmol. Vis. Sci. *35*, 9–32.

Young, R.W. (1985). Cell differentiation in the retina of the mouse. Anat. Rec. *212*, 199–205.